Effects of Chain Flexibility on Polymer Conformation in Dilute Solution Studied by Lattice Monte Carlo Simulation

Yunqi Li,[†,‡] Qingrong Huang,[‡] Tongfei Shi,*[,†] and Lijia An*[,†]

State Key Laboratory of Polymer Physics and Chemistry, Changchun Institute of Applied Chemistry, Chinese Academy of Sciences, Changchun 130022, P. R. China, and Department of Food Science, Rutgers University, 65 Dudley Road, New Brunswick, New Jersey 08901.

Received: May 28, 2006; In Final Form: September 15, 2006

Effects of chain flexibility on the conformation of homopolymers in good solvents have been investigated by Monte Carlo simulation. Bond angle constraint coupled with persistence length of polymer chains has been introduced in the modified eight-site bond fluctuation simulation model. The study about the effects of chain flexibility on polymer sizes reveals that the orientation of polymer chains under confinement is driven by the loss of conformation entropy.The conformation of polymer chains undergoing a gradual change from spherical iso-diametric ellipsoid to rodlike iso-diametric ellipsoid with the decrease of polymer chain flexibility in a wide region has been clearly illustrated from several aspects. Furthermore, a comparison of the freely jointed chain (FJC) model and the wormlike chain (WLC) model has also been made to describe the polymer sizes in terms of chain flexibility and quasi-quantitative boundary toward the suitability of the models.

Introduction

Persistence length (l_p) is a characteristic parameter that can describe the elastic properties and the chain flexibility of both synthetic and natural polymers. There are many reports on the persistence length and its characterization from different kinds of polymers in various environments.[1−4] In general, for a fully flexible polymer, the persistence length is in the order of several angstroms. But for a semi-flexible or rigid biopolymer, it can reach several hundred angstroms. For example, the l_p of poly(ethylene glycol) (PEG) is about 3.5 Å,[5] but the l_p of a single-stranded DNA or a double-stranded DNA is about 30 Å or 500 Å respectively.[6] A recent report suggests that the persistence length of DNA plays a key role in measuring the accurate self-replication.[7] The persistence length is an internal constraint for polymer chains, which also plays an important role on the dynamic properties of semi-flexible polymer chains.[8−10] The persistence length may be contributed by the steric repulsion-induced bare persistence length and the electrostatic persistence length.[11,12] In the theoretical treatment, the original definition of the persistence length l_p is written as[13]

$$l_p = -\frac{b}{\ln \cos \theta} \tag{1}$$

where b is the bond length and θ is the supplementary angle of the bond angle. The physical meaning of the persistence length and its relationship with the Kuhn length have been thoroughly discussed in the book of Rubinstein and Colby.[13]

From the experimental aspect, persistence length can be obtained from single molecular force spectroscopy,[14] the image of single molecule chain by atomic force microscopy (AFM),[15] light scattering,[16] and small-angle neutron scattering (SANS)[17] based on the physical models for polymer chains, such as the wormlike chain (WLC) model,[18,19] and the freely jointed chain (FJC) model.[20] The WLC model has been successfully used to describe rigid as well as semi-flexible polymer chains, such as DNA.[21−23] The FJC model affords a good understanding of flexible polymer chains, such as polysaccharides,[24] and synthetic polymers including polystyrene[25] and poly(vinyl alcohol),[26] etc. On the other hand, the nature of non-Gaussian distribution of monomers in polymer chains has been intensively investigated for a long time. These investigations on the conformation of polymer chains include the comparison of the relationship between size and shape of polymer chains using different chain models,[27] the effects of polymer−solvent interactions and chain lengths,[28,29] and the effects of the excluded volume of monomer,[30] etc. The equivalent ellipsoid model[28] is the most successful one in the description of size and shape of polymer chains. It has been used in the study of adsorption of protein-like polymer chains,[31] chain conformation transition of bovine serum albumin (BSA) with different surfactant concentrations,[32] SANS data of BSA at different pHs,[33] and the relationship between size and shape of branched polymer chains with different solvent qualities and number of arms.[34] On the theoretical aspect, Thirumalai and Ha used the mean-field variation approach to study the end-to-end distance distribution and elastic response of semi-flexible chains.[12] All these works are significant in exploring the nature behind polymer conformations, but further quasi-quantitative work covering a wide range of persistence lengths is still needed to understand the universal effects of the persistence length on the conformation of polymer chains in dilute solution.

Monte Carlo simulation is a powerful tool to obtain the information about polymer chains under the thermodynamic equilibrium state, especially for the intuitive description of polymer conformations. However, most of the traditional lattice Monte Carlo simulation models do not consider the persistence length constraint on polymer chains, and it is difficult to impose additional confinement on the simulation systems. In this paper,

* To whom correspondence should be addressed. E-mail: tfshi@ciac.jl.cn or ljan@ciac.jl.cn; Tel: +86−431−5262206; Fax: +86-431-5685653.

† Changchun Institute of Applied Chemistry, Chinese Academy of Sciences.

‡ Food Science Department, Rutgers University.

10.1021/jp0632790 CCC: $33.50
Published on Web 10/28/2006

we first introduce an improved eight-site bond fluctuation model,[35,36] which includes the persistence length constraint (i.e. bond angle constraint). We then discuss the effects of persistence length on the size and shape of the polymer chains. Finally, a comparison of the polymer sizes using WLC model and FJC model will be discussed.

Simulation Model

In three-dimension cubic lattice Monte Carlo simulation, the single-site model[37] and the eight-site model are the most widely used models. The eight-site model has the advantage of affording 108 possible bond vectors, 87 different bond angles, and 5 different bond lengths compared with 26 possible bond vectors, 14 different bond angles, and 3 different bond lengths afforded in the single-site model. The eight-site model shows more conformations, and makes the prediction of the simulation closer to the real polymer chains. The main disadvantage of the eight-site model is that it needs too many preprocessors on the space judgment before one trial of motion, which makes the source code very complex, and therefore reduces the executive efficiency in simulation processes.

To overcome these disadvantages of the traditional eight-site model, we improve this model by making an assumption that a monomer occupying a full small cube of eight sites is equal to the monomer locating at any of the eight sites in the cube with a co-equal probability of 1/8, which is based on the rule of "Translation Invariance" for a lattice with periodic boundary condition in all directions. Each site in a small cube of the simulation lattice can be recorded by a predetermined internal reference point of that small cube, which is used to record the position of that small cube. A random integer ranging from 1 to 8 is used to label the bias of the site from the internal reference point in this small cube.

To enhance the executive efficiency of the simulation and make this model extensible, an optimization in the method of recording the configuration of lattice during simulation has been employed. In this work, we use the array $V(n^*N, 4+k_c)$ to record the information of the polymer monomers, where n is the number of polymer chains, N is the number of monomers in each polymer chain (chain length), and k_c is the number of additional constraints imposed on polymer chains and contributed from each monomer. The four units for each column with the same index record the location of small cube and the random number ranging from 1 to 8. The matrix $S(L, L, L)$ is used to record all the information of the simulation lattice, and L is the side length of the lattice. All the eight sites in any small cube occupied by a monomer in the matrix $S(i, j, k)$ are assigned a value as

$$S(i,j,k) = n_P*10^m + N_P*10 + S_{ym} \quad (2)$$

where i, j, k determine the position in the matrix S, and n_P and N_P are the chain series and the monomer series in the n_Pth chain, respectively. S_{ym} is an integer between 0 and 9 that records the type of monomers. m is a constant integer, which satisfies

$$m \geq \{\text{int}\}[\log(N)] + 1 \quad (3)$$

Based on the above two improvements, the eight-site model becomes easier to manipulate, and turns out to be more efficient, partially due to a faster and longer sequence of random generator.[38] These improvements make the eight-site model easy to simulate up to 10 types of monomers in the system. Extra constraints on bond length, bond angle, torsion angle, and saturation contributed by each monomer can also be easily taken into consideration. In this work, the effects of bond angle constraint coupled with persistence length on the chain conformation in dilute homopolymer solution is studied using this newly developed eight-site bond fluctuation model.

The parameters used in this simulation are listed as: L is set to 100, and the periodic boundary condition is imposed on all directions to eliminate finite size effect. The number of polymer chains n is defined as $\phi L^3/N\upsilon$, where υ, which equals 8, is the number of lattice sites occupied by each monomer, or the excluded volume of each monomer. N is the chain length varying from 20 to 250. ϕ, which is fixed at 0.05, is the polymer concentration. The rest of sites are occupied by structureless solvent molecules with only one monomer. In this system, all the interactions are null except that the interaction pairs between the monomer in polymer chains and the solvent molecule have an attractive potential of $-0.1k_BT$, which makes good solvent for polymer chains. The cutoff of the interaction pair is $\sqrt{6}$.[39] The k_c equals one, and its corresponding position in the matrix $V(n^*N, 4+k_c)$ records the cosine value of the bond angle whose vertex is the monomer. For end monomers in each chain, their values are zero. In this way, the bond angle constraint can be easily recorded and controlled. All the polymer chains and solvent molecules are evenly dispersed in the simulation lattice, followed by 1×10^6 Monte Carlo steps (MCS) thermodynamic relaxation to achieve thermodynamic equilibrium state. Note that each MCS represents the time for each monomer in polymer chains to have one attempted motion. The relaxation motion includes a combination of bond-fluctuation[35] and snake-reptation[40] through the exchange of monomers in polymer chains with solvent molecules at the same time. The elemental attempted motion of the bond-fluctuation or the snake-reptation is (100) (i.e., one lattice site), and the snake-reptation only occurs when the random attempted motion is on the end monomer of a polymer chain. Both of the attempted motions follow the Metropolis sampling rule,[41] as well as the additional bond angle constraint. The acceptance probability for each motion can be written as

$$P_{acc} = P_{Metropolis}P_{bal} \quad (4)$$

where $P_{Metropolis}$ and P_{bal} are the acceptance probabilities satisfying the Metropolis rule[36] and the bond angle constraint, respectively. The latter is defined as:

$$P_{bal} = \exp[-W(\theta)/k_BT] \quad (5)$$

Here $W(\theta)$ is the potential function of bond angle, which is set as

$$W(\theta) = \begin{cases} \infty, & \theta > \theta_c \\ 0, & \theta \leq \theta_c \end{cases} \quad (6)$$

and

$$\theta_c = \text{acos}[\exp(-b/l_p)] \quad (7)$$

where b, which is equal to 2.688 (sites) length in this model, is the average bond length. This bond angle constraint is a little different to the work by Thirumalai and Ha,[12] where they studied the persistence length of chain with a fixed bond angle. To keep eqs 1 and 7 solvable, all the bond angles are limited to obtuse angles. The plot of the persistence length l_p versus the acceptance probability analyzed from bond angle constraint (F_{ba}) is shown in Figure 1, where F_{ba} is calculated by

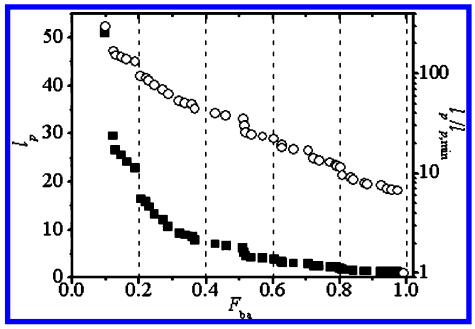

Figure 1. Plots of persistence length and its relative ratio versus the ideal acceptance probability under bond angle constraint. Persistence length (■) and their relative ratios (○).

$$F_{\mathrm{ba}} = \sum_{0<\theta\le\theta_c} n(\theta) / \sum_{\theta<\pi/2} n(\theta) \tag{8}$$

Here, $n(\theta)$ is the number of bond angles in all possible bond angles in the eight-site bond fluctuation model whose values are equal to θ. Figure 1 shows that, although the absolute persistence length cannot reach a larger value, its relative ratio ($l_p/l_{p,\min}$) affords a two-order magnitude change with an applicable acceptance probability from bond angle constraint, where $l_{p,\min}$ is the minimum persistence length which corresponds to the minimum obtuse angle in this model, and chains with the persistence length of $l_{p,\min}$ are regarded as fully flexible chains. These results indicate that our model can cover from fully flexible polymers (l_p of several angstroms) to rigid polymers (l_p of several hundred angstroms). Therefore, this improved simulation method will afford an opportunity to understand the complex properties and behaviors of biopolymers from the well-developed polymer physics theories for synthetic polymers.

Results and Discussion

As the first application of this improved eight-site bond fluctuation model, the simulation efficiency including the simulation time and the simulation acceptance probability must be tested. The reduced internal energy factor α, which is defined in eq 9, has been calculated to determine whether the sample has reached the thermodynamic equilibrium state.

$$\alpha(t) = \frac{\langle U(t)U(0)\rangle}{\langle U(0)\rangle^2} \tag{9}$$

where $U(t)$ is the total interaction energy of each chain at the simulation time of t, and the $\langle\ \rangle$ denotes the ensemble average in the simulation sample. Figure 2a shows the plots of α(t) versus t in a semilogarithm coordinate for fully flexible polymers with different chain lengths. It can be seen that the relaxation time to reach the thermodynamic equilibrium state is about 1×10^5 MCS in this simulation, and monotonically increases as the chain length increases. This result indicates that the total simulation time of 1×10^6 MCS is long enough to obtain configurations under thermodynamic equilibrium. The acceptance probability of the bond angle constraint versus persistence length at different chain lengths is plotted and compared with the ideal case (data from Figure 1), as shown in Figure 2b. This result suggests that the additional bond angle constraint can maintain the feature of the simulation method.

To characterize the conformation of polymer chains in dilute solution, several parameters relevant to the size of polymer chains, including the radius of gyration R_g, the hydrodynamic radius R_h, and the end-to-end distance R_F are used. The R_h for

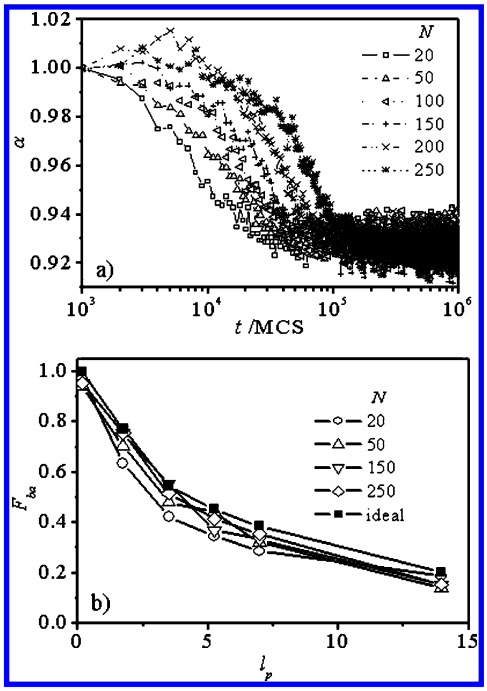

Figure 2. (a) Reduced energy factor evolutes with Monte Carlo Steps (MCS) for fully flexible chains ($l_p = 0.17$) with different chain lengths, and (b) persistence length dependence of the acceptance probability for polymers of different chain lengths.

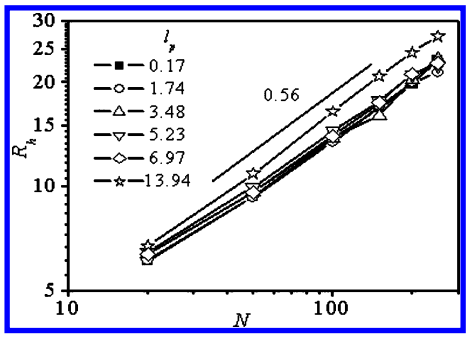

Figure 3. Scaling relationship between the hydrodynamic radius R_h and polymer chain length at different chain flexibilities. Note that the radius of gyration R_g has the similar scaling exponent with chain length as R_h, thus is not shown again.

linear polymer chains in dilute solution can be calculated by[30]

$$R_h = \left\{ \frac{1}{N^2} \sum_{i\neq j}^{N} \left\langle \frac{1}{|\vec{r}_i - \vec{r}_j|} \right\rangle \right\}^{-1} \tag{10}$$

where $\vec{r}_i$ is the position of the ith monomer in a polymer chain. The R_h has similar chain length dependence with N as R_g, which is calculated through as follows:

$$R_g = \left\{ \frac{1}{N^2} \left\langle \sum_{i,j}^{N} (\vec{r}_i - \vec{r}_j)^2 \right\rangle \right\}^{1/2} \tag{11}$$

Both R_g and R_h well satisfy the scaling relationship of $R_h \propto R_g \propto N^\nu$ with $\nu = 0.588$ for polymer chains in dilute solution under good solvent condition, and the persistence length does not affect this scaling relationship, as shown in Figure 3 (the scaling results of R_g are not shown).

To give a clear statement of the conformation of polymer chains, the end-to-end distance R_F is also calculated according to the following definition:

$$R_F = \langle |\vec{r}_1 - \vec{r}_N|^2 \rangle^{1/2} \quad (12)$$

The general feature of the chain flexibility effect on the polymer conformations in dilute solution can be expressed from the parameters R_g/R_h and R_g/R_F. Their dependence on the chain flexibility l_p/N_c is shown in Figure 4, where N_c is the ensemble-averaged contour length of polymer chains obtained through the relationship:

$$N_c = \langle \sum_{i=1}^{N-1} |\vec{r}_{i+1} - \vec{r}_i| \rangle \quad (13)$$

The R_g/R_h, which equals 1.45 for fully flexible chains in good solvent, is in good agreement with the theoretical prediction.[13] R_g/R_h increases to about 2.11 for rigid chains as the chain flexibility decreases, showing a rodlike chain behavior.[42] The R_g/R_F changes from 0.60 (1 for perfect spherical coil) through 0.41 (Gaussian coil) to 0.29 (rodlike chain), which provides a directly evidence for the change of conformation from spherelike to rodlike. Particularly, when R_g/R_F equals 0.29 for a rodlike conformation, the long axis can be about 8-fold of the shorter one, which is about 4-fold of the ideal radius of gyration of polymer chains (R_{g0}) under the assumption that the distribution of monomers in each polymer chain is in an ellipsoidal shape.[28] It suggests that, if polymer chains are confined in a slit narrower than about $4R_{g0}$, the conformation entropy of polymer chains must suffer from the confinement. This result is coincident with the observation by Schaub, who observed the complete segregation of chain ends when the thickness of film was less than $4R_{g0}$.[43] On the other hand, semi-flexible polymer chains with different persistence length may exhibit interesting behaviors, such as the orientation of polymer chains when the persistence length is larger than the width of the confining microchannel,[44] and the change in the chain conformation transition on surface.[45] From our result, one notes that the orientation of semi-flexible polymer chains under confinement at about 2~6 R_{g0} may be driven by the loss of conformation entropy of the polymer chains.[46−48]

A more accurate description for the gradual conformation changes from spherical coil to rodlike chain with the decrease of chain flexibility can be related to the ellipsoidal distribution model,[49] which can be extrapolated to a cigar model in two-dimension.[50] According to this ellipsoid model,[51] the monomer has a wide distribution along the end-to-end direction. L_1^2, L_2^2, and L_3^2 are used to record the accumulation of monomer distribution on three orthogonal directions predetermined by the end-to-end vector, $_F$. They are obtained from

$$L_1^2 = \langle \sum_{i=1}^{N} \{[(\vec{r}_i - \vec{r}_{cm}) \bullet \vec{e}_{//}]^2\} \rangle \quad (14a)$$

$$L_2^2 = \langle \sum_{i=1}^{N} \{[(\vec{r}_i - \vec{r}_{cm}) \bullet (\vec{e}_{//} \times \vec{e}_{\perp})]^2\} \rangle \quad (14b)$$

$$L_3^2 = \langle \sum_{i=1}^{N} \{[(\vec{r}_i - \vec{r}_{cm}) \bullet (\vec{e}_{//} \times (\vec{e}_{//} \times \vec{e}_{\perp}))]^2\} \rangle \quad (14c)$$

where $\vec{e}_{//} // \vec{R}_F$ and $\vec{e}_{\perp} \perp \vec{R}_F$ are unit vectors, $\vec{r}_{cm}$ is the position of the center of mass of the polymer chain, and the $\langle\ \rangle$ denotes the ensemble average. Because $\vec{e}_{\perp}$ is quite arbitrary, we set $L_1^2 \geq L_2^2 \geq L_3^2$. Then the three accumulation quantities are reduced to show whether the conformation is spherelike, disklike, or rodlike. They are defined as

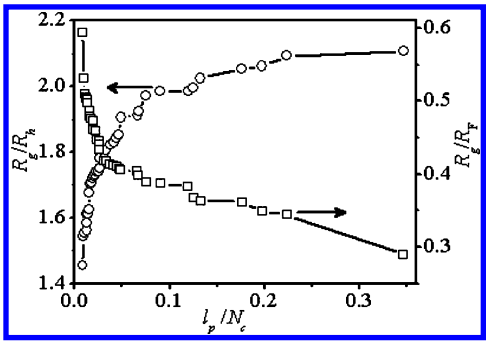

Figure 4. Dependence of the R_g/R_h (□), and R_g/R_F (○) on the chain flexibility l_p/N_c.

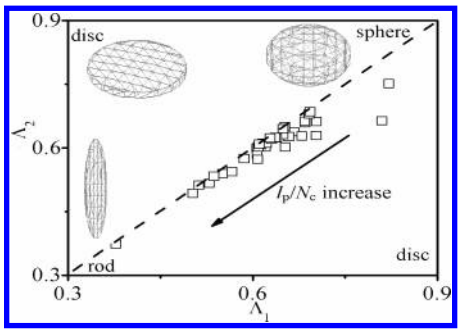

Figure 5. Chain conformation changes with chain flexibility, as illustrated by the plot of Λ_2 versus Λ_1.

$$\Lambda_1 = L_2^2/L_1^2 \quad (15a)$$

$$\Lambda_2 = L_3^2/L_1^2 \quad (15b)$$

The two parameters relate the conformation as: (i) spherelike when $\Lambda_1 \cong \Lambda_2 \rightarrow 1$; (ii) rodlike when $\Lambda_1 \cong \Lambda_2 \rightarrow 0$; (iii) disklike when $\Lambda_1 \ll \Lambda_2$ *or* $\Lambda_1 \gg \Lambda_2$, and the smaller one tends to be zero. Figure 5 clearly indicates that the conformation changes from spherelike to rodlike through prolate isodiametric ellipsoid as the values of Λ_1 or Λ_2 change from 0.9 to 0.3. This result covers some previous reports,[28,30] and clearly shows an intuitive picture on how the chain flexibility affects the conformation of polymer chains in a wide flexibility range.

It is known that the WLC model is more suitable to describe semi-flexible and rigid polymer chains than the FJC model. However, to the best of our knowledge, there is no quasi-quantitative boundary reported that can be used to evaluate which model is better for describing the characters of polymer chains with a specific range of chain flexibilities. Here, a comparison of two models from the simulation results is presented by calculating the end-to-end distance R_F. From the standard WLC model, $R_{F,WLC}$ can be obtained from[13]

$$R_{F,WLC} = \left\{ 2l_p^2 \left[\frac{N_c}{l_p} - 1 + \exp\left(-\frac{N_c}{l_p} \right) \right] \right\}^{1/2} \quad (16)$$

whereas $R_{F,\ FJC}$, which equals $N^{\nu}b$, is simply obtained from the FJC model. The plots of the ratios $R_{F,WLC}/R_F$ and $R_{F,FJC}/R_F$ versus l_p/N_c are shown in Figure 6. Here, R_F is directly accumulated from the simulation system using eq 12. It can be seen that both $R_{F,WLC}/R_F$ and $R_{F,FJC}/R_F$ decrease as the chain flexibility decreases (i.e., l_p/N_c increases). When $R_{F,FJC}/R_F$ equals 1, the l_p/N_c for FJC model is 0.012, polymer chains are close to Gaussian coil. When $R_{F,WLC}/R_F$ equals 1, the l_p/N_c for WLC model is 5.41 by extrapolation of the curve fitting to the data

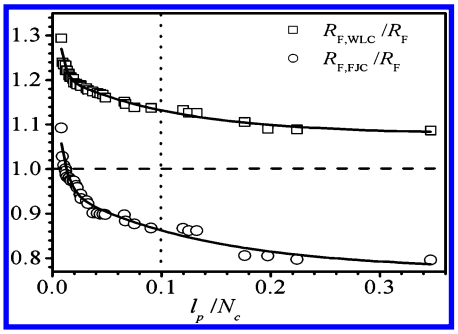

Figure 6. Comparison of the wormlike chain (WLC) model and the freely jointedchain (FJC) model using the plots of the ratios of $R_{F,WLC}/R_F$ and $R_{F,FJC}/R_F$ versus the polymer chain flexibility (l_p/N_c). The vertical dot lines label the quasi-quantitative boundary of chain flexibility, and the solid curves through the simulation data are used to guide the eyes.

from WLC model (figure not shown), polymer chains are very rigid in this case. FJC model can well predict R_F when l_p/N_c is smaller than about 0.1, while WLC model can well predict R_F in rest of the flexibility range, as shown in Figure 6. In the medium flexibility range where l_p/N_c is about 0.1, both of FJC model and WLC model predictions show about 15% error, which is quite large. The reason may be that it is the turn-round length, rather than the persistence length, that can serve as a good parameter to describe the mesogenicity of the real molecule, as suggested by Crawshaw and Windle.[52]

Summary

The Monte Carlo simulation model to describe the eight-site bond fluctuation has been modified and developed to study the effects of chain flexibility on the conformation of polymer chains in dilute solution. The conformation of polymer chains changing from spherelike to rodlike with the decrease of chain flexibility has been clearly illustrated, and the orientation of semi-flexible polymer chains under confinement has been interpreted as a result of loss of conformation entropy. Two physical models for polymer chains, freely jointed chain (FJC) model and wormlike chain (WLC) model, have been compared. It is found that, according to the chain flexibility l_p/N_c, the boundary to select the optimum model between FJC model and WLC model is about 0.1. FJC model is better when l_p/N_c is smaller than this boundary, while WLC model works better in rest of the chain flexibility range.

Acknowledgment. We thank P. K. Dutta of MNNIT, Allahabad, India for proof-reading of the manuscript. This work is supported by ACS-PRF (41333-G7), the National Natural Science Foundation of China (20334010, 50503022, 50390090, 50340420392, and 20620120105) Programs and the Chinese Academy of Sciences (KJCX2-SW-H07), and subsidized by the Special Funds for National Basic Research Program of China (2003CB615600).

References and Notes

(1) Manning, G. S. *Biopolymers* **1988**, *27*, 1529−1542.
(2) Ott, A.; Magnasco, M.; Simon, A.; Libchaber, A. *Phy. Rev. E* **1993**, *48*, R1642−1645.
(3) MacKintosh, F. C.; Käs, J.; Janmey, P. A. *Phys. Rev. Lett.* **1995**, *75*, 4425−4428.
(4) Round, A. N.; Berry, M.; McMaster, T. J.; Stoll, S.; Gowers D.; Corfield, A. P.; Miles, M. J. *Biophys. J.* **2002**, *83*, 1661−1670.
(5) Movileanu, L.; Bayley, H. *PNAS* **2001**, *98*, 10137−10141.
(6) Austin, R. *Nat. Mater.* **2003**, *2*, 567−568.
(7) Kuznetsov, S. V.; Shen, Y.; Benight, A. S.; Ansari A. *Biophys. J.* **2001**, *81*, 2864−2875.
(8) Harnau, L.; Winkler, R. G.; Reineker, P. *J. Chem. Phys.* **1997**, *106*, 2469−2476.
(9) Winkler, R. G. *J. Chem. Phys.* **2003**, *118*, 2919−2928.
(10) Kroy, K.; Frey, E. *Phys. Rev. Lett.* **1996**, *77*, 306−309.
(11) Kayitmazer, A. B.; Shaw, D.; Dubin, P. L. *Macromolecules* **2005**, *38*, 5198−5204.
(12) Thirumalai, D.; Ha, B.-Y. *Theoretical and Mathematical Models in Polymer Research*; Grosberg, A. Y., Ed.; Academic Press: New York, 1998; pp 1−35.
(13) Rubinstein, M.; Colby, H. *Polymer Physics*; Oxford University, New York, 2004.
(14) Nishida, K.; Kaji, K.; Kanaya, T.; Shibano, T. *Macromolecules* **2002**, *35*, 4084−4089.
(15) van Noort, J.; van der Heijden, T.; de Jager, M.; Wyman, C.; Kanaar, R.; Dekker: C. *PNAS* **2003**, *100*, 7581−7586.
(16) Cuppo, F.; Reynaers, H.; Paoletti, S. *Macromolecules* **2002**, *35*, 539−547.
(17) Cola, E. D.; Waigh, T. A.; Trinick, J.; Tskhovrebova, L.; Houmeida, A.; Hintzen, W. P.; Dewhurst, C. *Biophys. J.* **2005**, *88*, 4095−4106.
(18) Kratky, O.; Porod, G. *Recl. Trav. Chim.* **1949**, *68*, 1106−1122.
(19) Wang, M. D.; Yin, H.; Landick, R.; Gelles, J.; Block, S. M. *Biophys. J.* **1997**, *72*, 1335−1346.
(20) Smith, S. B.; Cui, Y.; Bustamanate, C. *Science* **1996**, *271*, 795−799.
(21) Janshoff, A.; Neitzert, M.; Oberdörfer, Y.; Fuchs, H. *Angew. Chem., Int. Ed.* **2000**, *39*, 3212−3237.
(22) Bustamante, C.; Smith, S. B.; Liphardt, J.; Smith, D. *Curr. Opin. Struct. Biol.* **2000**, *10*, 279−285.
(23) Rosa, A.; Hoang, T. X.; Marenduzzo, D.; Maritan, A. *Biophys. Chem.* **2005**, *115*, 251−254.
(24) Marszalek, P. E.; Oberhauser, A. F.; Pang, Y. P.; Fernandez, J. M. *Nature (London)* **1998**, *396*, 661−664.
(25) Kikuchi, H.; Yokoyama, N.; Kajiyama, T. *Chem. Lett.* **1997**, *26*, 1107−1108.
(26) Li, H.; Zhang, W.; Zhang, X.; Shen, J.; Liu, B.; Gao, C.; Zou, G. *Macromol. Rapid Commun.* **1998**, *19*, 609−611.
(27) Benoit, H.; Doty, P. *J. Phys. Chem.* **1953**, *57*, 958−963.
(28) Solc K. *J. Chem. Phys.* **1971**, 55, 335−344; Solc, K.; Stockmayer, W. H. *J. Chem. Phys.* **1971**, *54*, 2756−2757.
(29) Tanaka, G.; Mattice, W. L. *Macromol. Theory Simul.* **1996**, *5*, 499−523.
(30) Steinhauser, M. O. *J. Chem. Phys.* **2005**, *122*, 094901.
(31) Sun, T.; Zhang, L. *Polymer* **2005**, *46*, 5714−5722.
(32) Lee, C. T., Jr.; Smith, K. A.; Hatton, T. A. *Biochemistry* **2005,** *44*, 524−536.
(33) Bendedouch, D.; Chen, S.-H. *J. Phys. Chem.* **l983**, *87*, 1473−1477.
(34) Zifferer, G. *Macromol. Theory Simul.* **1999**, *8*, 433−462.
(35) Carmesin, I.; Kremer K. *Macromolecules* **1988**, *21*, 2819−2823.
(36) Deutsch, H. P.; Binder, K. *J. Chem. Phys.* **1991**, *94*, 2294−2304.
(37) Verdierand, P. H.; Stockmayer, W. H. *J. Chem. Phys.* **1962**, *36*, 227−235.
(38) L'cuyer, P. *Commun. ACM* **1988**, *31*, 742−774.
(39) Wilding, N. B.; Müller M.; Binder K. *J. Chem. Phys.* **1996**, *105*, 802−809.
(40) Binder, K.; Heermann, D. W. *Monte Carlo Simulation in Statistical Physics*; Springer-Verlag: New York, 1992.
(41) Metropolis, N.; Rosenbluth, A. W.; Rosenbluth, M. N.; Teller A. H. *J. Chem. Phys.* **1953**, *21*, 1087−1092.
(42) Nie, T.; Zhao, Y.; Xie, Z.; Wu, C. *Macromolecules* 2003, *36*, 8825−8829.
(43) Schaub, T. F., Jr. Master thesis, MIT, 1995.
(44) Granick, S.; Kumar, S. K.; Amis, E. J.; Antonietti, M.; Balazs, A. C.; Chakraborty, A. K.; Grest, G. S.; Hawker, C.; Janmey, P.; Kramer, E. J.; Nuzzo, R.; Russell, T. P.; Safinya, C. R. *J. Polym. Sci., Part B: Polym. Phys.* **2003**, *41*, 2755−2793.
(45) Edvinsson, T. *Comprehensive Summaries of Uppsala Dissertations*; Acta Universitatis Upsaliensis: Uppsala, 2002.
(46) Cordeiro, C. E.; Molisana, M.; Thirumalai, D. *J. Phys. II* **1997**, *7*, 433−447.
(47) van Vliet, J. H.; Luyten, M. C.; ten Brinke, G. *Macromolecules* **1992**, *25*, 3802−3806.
(48) Nie, Z. H.; Su, Z. H..; Sun, Z. Y.; Shi, T. F.; An, L. J. *Macromol. Theory Simul.* **2005**, *14*, 463−473.
(49) Teraoka, I. *Polymer Solutions: An Introduction to Physical Properties*; John Wiley & Sons: New York, 2002.
(50) Pakula, T. *J. Chem. Phys.* **1991**, *95*, 4685−4690.
(51) Note, the ellipsoid model used here (see ref 42) is a little different from that proposed by Solc and Stockmayer (ref 28). The difference is in the determination of the principle extension. Here, the principle extension is assumed to be parallel to the end-to-end vector directly rather than an instant accumulation of the moment to the radius of gyration as defined in ref 28.
(52) Crawshaw, J.; Windle, A. H. *Fibre Diffr. Rev.* **2003**, *11*, 52−67.